A Letters Journal Exploring the Frontiers of Physics

December 2019

EPL, **128** (2019) 67002 www.epljournal.org
doi: 10.1209/0295-5075/128/67002

Superconductivity at 4.6 K in the Cr-based nitride $La_3Cr_{10-x}N_{11}$

Y. J. Li[1,2], W. Wu[1,2(a)], K. Liu[3], Z.-H. Yu[4], D. S. Wu[1,2], Y. T. Shao[1,2], S. H. Na[1,2], G. Li[1,5], P. Zheng[1], T. Xiang[1,2,6] and J. L. Luo[1,2,5(b)]

[1] *Beijing National Laboratory for Condensed Matter Physics and Institute of Physics, Chinese Academy of Sciences Beijing 100190, China*
[2] *School of Physical Sciences, University of Chinese Academy of Sciences - Beijing 100190, China*
[3] *Department of Physics and Beijing Key Laboratory of Opto-electronic Functional Materials and Micro-nano Devices, Renmin University of China - Beijing 100872, China*
[4] *School of Physical Science and Technology, ShanghaiTech University - Shanghai 201210, China*
[5] *Songshan Lake Materials Laboratory - Dongguan, Guangdong 523808, China*
[6] *Kavli Institute for Theoretical Sciences - Beijing 100190, China*

received 2 November 2019; accepted in final form 7 January 2020
published online 4 February 2020

PACS 74.70.-b – Superconducting materials other than cuprates
PACS 74.25.-q – Properties of superconductors
PACS 71.27.+a – Strongly correlated electron systems; heavy fermions

Abstract – A new Cr-based superconductor is discovered in cubic nitride $La_3Cr_{10-x}N_{11}$, which is isostructural with $Pr_3Cr_{10-x}N_{11}$. A cubic crystal structure of $La_3Cr_{10-x}N_{11}$ was determined by single-crystal X-ray diffraction. The superconducting transition temperature T_c from resistivity measurement is 4.6 K, while magnetization and specific heat measurements confirm its bulk property. The upper critical field of H_{c2} is about 12.2 T, exceeding the Pauli paramagnetic limit. It is found that the crystallinity and stoichiometry of the samples play important roles in the observation of superconductivity in $La_3Cr_{10-x}N_{11}$.

Introduction. – Since the discovery of the chromium-based superconductor CrAs [1–3] with superconductivity at 2 K under an external pressure of 1 GPa, chromium-based superconductors have attracted a great deal of attention. Recently, quasi one-dimensional (Q1D) $A_2Cr_3As_3$ and ACr_3As_3 (A =Na, K, Rb, Cs) [4–10] were reported, exploring those quasi one-dimensional superconductors is a hot spot primarily owing to their reduced dimensionality, significant electron correlations, and possible unconventional superconductivity. Up to now, there are only few chromium-based superconductors at either ambient or elevated pressure, since it is difficult to suppress the magnetic moment of the Cr ion and the proximity to magnetic order.

Very recently, superconductivity was observed in $Pr_3Cr_{10-x}N_{11}$ with $T_c \sim 5.25$ K [11]. This compound has a large electronic specific-heat coefficient of 170 mJ/mol K^2, about 10 times larger than that estimated by band structure calculations, which suggests that the effective mass is much enhanced and correlation among $3d$ electrons is very strong in $Pr_3Cr_{10-x}N_{11}$. A relatively large upper critical field at the zero-temperature limit, $H_{c2}(0)$ is about 12.6 T, larger than the Pauli limit of paramagnetic pair-breaking field. Those results demonstrate that $Pr_3Cr_{10-x}N_{11}$ is the first Cr-based superconductor discovered in chromium nitrides with strong electron correlations.

A series of isostructural compounds $Ln_3Cr_{10-x}N_{11}$ (Ln = La, Ce, Pr) was firstly synthesized by Broil *et al.* in 1995 [12]. It contains 192 atoms in a face-centered cubic unit cell with three kinds of building blocks as shown in fig. 1(a). The building blocks are La_6N_9, Cr_8N_{13} and Cr_6. The space group is $Fm\bar{3}m$ (No. 225) with lattice constants $a = 12.982(1)$ Å, 12.843(1)–12.861(3) Å, and $a = 12.891(2)$ Å for $La_3Cr_{10-x}N_{11}$, $Ce_3Cr_{10-x}N_{11}$, and $Pr_3Cr_{10-x}N_{11}$, respectively, which were determined by the rare earth elements [12]. The lattice constant of $Ce_3Cr_{10-x}N_{11}$ is slightly smaller than that of $Pr_3Cr_{10-x}N_{11}$, which might be associated with the mixed valence behavior of the cerium atoms in this compound. It is our interest to explore by substituting rare

(a) E-mail: Welyman@iphy.ac.cn (corresponding author)
(b) E-mail: jlluo@iphy.ac.cn (corresponding author)

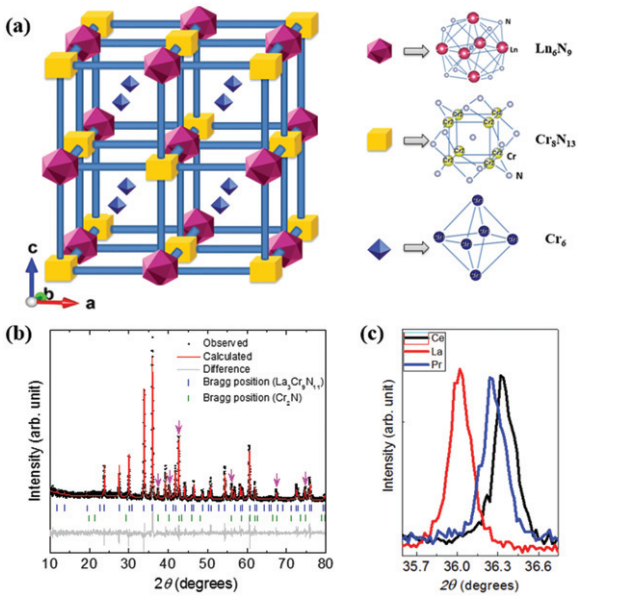

Fig. 1: (a) The face-centered cubic cell of $La_3Cr_{10-x}N_{11}$ with 3 types of building blocks La_6N_9, Cr_8N_{13} and Cr_6, respectively. The blocks are shown in a shrunken form [11]. (b) GSAS fit of room temperature powder X-ray diffraction data for $La_3Cr_{10-x}N_{11}$ indexed to space group $Fm\bar{3}m$. (c) The main [333] peak of $Ln_3Cr_{10-x}N_{11}$ (Ln = La, Ce, Pr) samples.

earth element of $Pr_3Cr_{10-x}N_{11}$ thereby varying the Cr-Cr distance, whether the superconducting properties could be altered [13].

Here, we report the observation of superconductivity in $La_3Cr_{10-x}N_{11}$ with $T_c \sim 4.6$ K. The samples of $La_3Cr_{10-x}N_{11}$ have a shielding fraction of 60% at 2 K from zero-field cooling (ZFC) magnetic susceptibility and an obvious superconducting anomaly from specific heat measurements. A relatively large upper critical field is found at the zero-temperature limit, $H_{c2}(0) \sim 12.2$ T, which is larger than the Pauli paramagnetic pair breaking field. From the band calculation, we find that the density of states at the Fermi energy are contributed mainly by Cr 3d electrons in $La_3Cr_{10-x}N_{11}$. Comparing to $La_3Cr_{10-x}N_{11}$ and $Pr_3Cr_{10-x}N_{11}$, however, $Ce_3Cr_{10-x}N_{11}$ shows no signature of superconductivity down to 1.8 K.

Experiments and calculations. – The synthesis method of $Ln_3Cr_{10-x}N_{11}$ (Ln = La, Ce, Pr) samples were reported in the literature [12] by direct reactions of the corresponding binary nitrides, staring with LnN (99%) and a mixture of the chromium nitrides (CrN and Cr_2N) in a mass ratio of 3:7, which is determined by the percentage of CrN in the mixture of chromium nitrides. The operations were all performed in an Ar-filled glovebox with water and oxygen content below 0.1 ppm since LnN is easily oxidized to Ln_2O_3. Cold-pressed pellets of the mixtures were sealed in an evacuated quartz tube. The pellets were gradually heated to 1000 °C and kept at the temperature for 50 h, followed by furnace cooling to room temperature. The products were reground, pressed into pellets, and heated in evacuated quartz tube to 1165 °C and held for 120 hours. Synthesized powder is air sensitive, so it is important to avoid exposure to air as much as possible while handling samples.

Powder X-ray diffraction (XRD) experiments were conducted at room temperature by a PANalytical X-ray diffractometer with Cu $K_{\alpha 1}$ radiation. The XRD pattern of $La_3Cr_{10-x}N_{11}$ was analyzed with Rietveld refinement using the GSAS program package with a user interface EXPGUI [14]. The electrical resistivity and specific heat were measured in a quantum design physical property measurement system (PPMS-9) by the standard four-probe method and relaxation method, respectively. The DC susceptibility was measured in a quantum design SQUID VSM under zero-field-cooling (ZFC) and field-cooling (FC) modes.

First-principles electronic structure calculations on $Ln_3Cr_{10-x}N_{11}$ (Ln = La, Ce, Pr) were performed with the projector augmented wave (PAW) method [15,16] as implemented in the VASP package [17–19]. The generalized gradient approximation (GGA) of Perdew-Burke-Ernzerhof (PBE) type [20] was adopted for the exchange-correlation functional. The kinetic energy cutoff of the plane-wave basis was set to be 520 eV. A $6 \times 6 \times 6$ k-point mesh was employed for the Brillouin zone sampling of the primitive cell, which contains two formula units (f.u.) (see inset of fig. 6). The Gaussian smearing method with a width of 0.05 eV was used for the broadening of Fermi surface. The on-site Coulomb repulsion among localized d or f electrons was included by using the GGA+U formalism of Dudarev *et al.* [21]. The values of effective Hubbard U for Ln $4f$ and Cr $3d$ electrons were set to 5.0 eV and 3.0 eV, respectively. The lattice constants of $Ln_3Cr_{10-x}N_{11}$ (Ln = La, Ce, Pr) were fixed at their corresponding experimental values of 12.982(1), 12.861(3), and 12.891(2) Å. The Cr vacancy was studied by subtracting real Cr atom from the primitive cell. The internal atomic positions were allowed to relax until the forces on all atoms were smaller than 0.01 eV/Å.

Results and discussions. – Figure 1(b) shows the GSAS refinement of $La_3Cr_{10-x}N_{11}$ under ambient condition (the detailed refined structural parameters are listed in table S1 of the Supplementary Material `Supplementarymaterial.pdf` (SM)), which indicates that $La_3Cr_{10-x}N_{11}$ crystallized in face-centered cubic (FCC) structure with space group $Fm\bar{3}m$. All the $La_3Cr_{10-x}N_{11}$ reflections can be well indexed based on a cubic cell with lattice parameters $a = 12.9535$ Å, consistent with those reported in the literature ($a = 12.982(1)$ Å) [12], indicating their ideal composition. A small amount of raw reactant Cr_2N existed in materials. The diffraction angles were calculated from the lattice parameters obtained by the least-squares fitting method. Figure 1(c) shows the main peak of [333] about $Ln_3Cr_{10-x}N_{11}$ (Ln = La, Ce, Pr) samples, the shift of peak is consistent with the change of lattice constants.

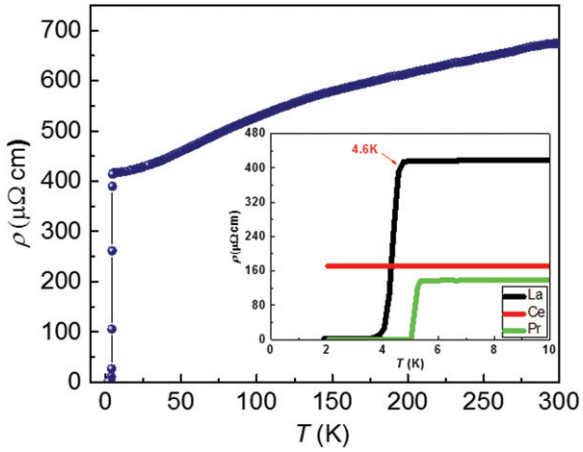

Fig. 2: Temperature dependence of electrical resistivity for $La_3Cr_{10-x}N_{11}$ from 1.9 K to 300 K at zero field. The inset shows the resistivity for $Ln_3Cr_{10-x}N_{11}$ (Ln = La, Ce, Pr) below 10 K.

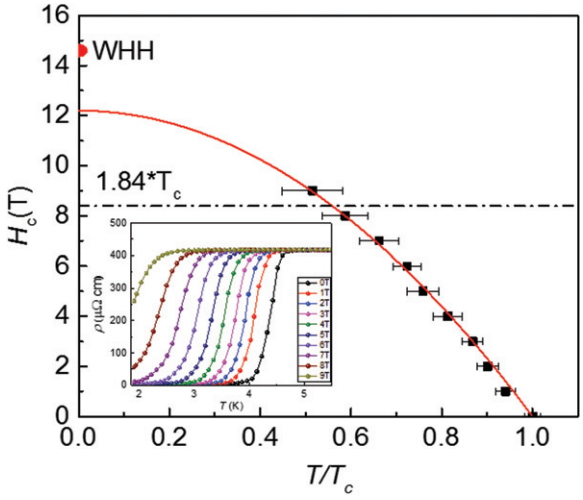

Fig. 3: Temperature dependence of upper critical field $H_{c2}(T)$ yields $H_{c2}(0) \sim 12.2$ T. The Pauli limit for H_{c2} is marked by the horizontal line. Inset shows the resistivity measurements under different magnetic fields up to 9 T.

Figure 2 shows the temperature dependence of electrical resistivity for $La_3Cr_{10-x}N_{11}$ from 1.9 K to 300 K at zero field. The normal state resistivity is metallic, with no abrupt change observed. Resistivity can be fitted by T^2 relation from 5 K to 75 K, indicating a Fermi liquid behavior. At low temperatures, a sharp superconducting transition is observed with onset T_c about 4.6 K and zero resistivity at 3.7 K. The superconducting transition width is 0.86 K as a result of poor crystallinity (see fig. S1 in the SM for details) compared to $Pr_3Cr_{10-x}N_{11}$. The inset of fig. 2 shows the resistivities for $Ln_3Cr_{10-x}N_{11}$ (Ln = La, Ce, Pr). $La_3Cr_{10-x}N_{11}$ shows superconductivity at 4.6 K, lower than $Pr_3Cr_{10-x}N_{11}$ with $T_c \sim 5.25$ K. The T_c of $La(Pr)_3Cr_{10-x}N_{11}$ is close to $K_2Cr_3As_3$ with $T_c \sim 6.1$ K [4], no superconductivity was observed in $Ce_3Cr_{10-x}N_{11}$ above 1.8 K.

$La_3Cr_{10-x}N_{11}$ shows a similar upper critical field with $Pr_3Cr_{10-x}N_{11}$ [11]. The inset of fig. 3 shows resistivity data under different magnetic fields up to 9 T. The transition temperature T_c shifts to lower temperature and the transition width is gradually broadened with increasing the magnetic field. At low magnetic field, $|dH_{c2}/dT|$ is found to be 4.7 T/K, which is about 2/3 of that of $K_2Cr_3As_3$. At the highest measured field of 9 T, the onset superconducting transition temperature is 2.4 K, just 2.2 K less than zero field T_c. This means zero temperature upper critical field $H_{c2}(0)$ should be much larger than 9 T, which is relatively large comparing to its superconducting transition temperature. The upper critical field $H_{c2}(0)$ can be estimated with the formula

$$H_{c2}(T) = H_{c2}(0)\left(1 - t^2\right), \qquad (1)$$

where t is the reduced temperature $t = T/T_C$. By fitting, we obtained $H_{c2}(0) \sim 12.2$ T and 14.9 T with the Werthamer-Helfand-Honenberg (WHH) formula [22]

$$\mu_0 H_{c2}(0) = -0.693 T_C \left(\frac{\mathrm{d}\mu_0 H_{c2}(T)}{\mathrm{d}T}|_{T_C}\right). \qquad (2)$$

On the other hand, the Pauli paramagnetic limit for the upper critical field is $H_P = 1.84 T_C \approx 8.46$ T in the case of isotropic full superconducting gap without considering spin-orbit coupling [23,24]. Taking $\mu_0 H_{c2}(0) = 12.2$ T as the upper limit, the $\mu_0 H_{c2}(0)$ of $La_3Cr_{10-x}N_{11}$ is 145% as large as H_P. In some case, the upper critical magnetic field $\mu_0 H_{c2}(0)$ may serve as a possible indicator for unconventional superconductivity. The high superconducting upper critical field could be originated from multi-bands effects [25], the strong coupling effect [26], the spin-triplet pairing [27], and the strong spin-orbit coupling effect in low-dimensional systems [22,28]. The origin of large $H_{c2}(0)$ in $La_3Cr_{10-x}N_{11}$ needs to be further studied. The obtained $\mu_0 H_{c2}(0)$ allows us to estimate the Ginzburg-Landau coherence length according to the relation [29]

$$\mu_0 H_{c2}(0) = \Phi_0 / 2\pi\xi_{GL}^2, \qquad (3)$$

where Φ_0 is the quantum flux $h/2e$ and $\xi_{GL}(0) = 51.96$ Å.

The bulk superconductivity in $La_3Cr_{10-x}N_{11}$ was confirmed by DC magnetic susceptibility measurements. Figure 4(a) shows susceptibility χ under a magnetic field of 20 Oe from 1.9 K to 7 K in both ZFC and FC processes. χ starts to drop below T_C and the diamagnetic signal tends to saturate at low temperatures. The shielding fraction is close to 60% at 2 K as estimated from ZFC data. Figure 4(b) shows that the normal state susceptibility χ of $La_3Cr_{10-x}N_{11}$ is Pauli paramagnetic with nearly a temperature-independent susceptibility similar to the previous report [12]. Compared with $La_3Cr_{10-x}N_{11}$, χ of $Pr_3Cr_{10-x}N_{11}$ increases with decreasing temperature,

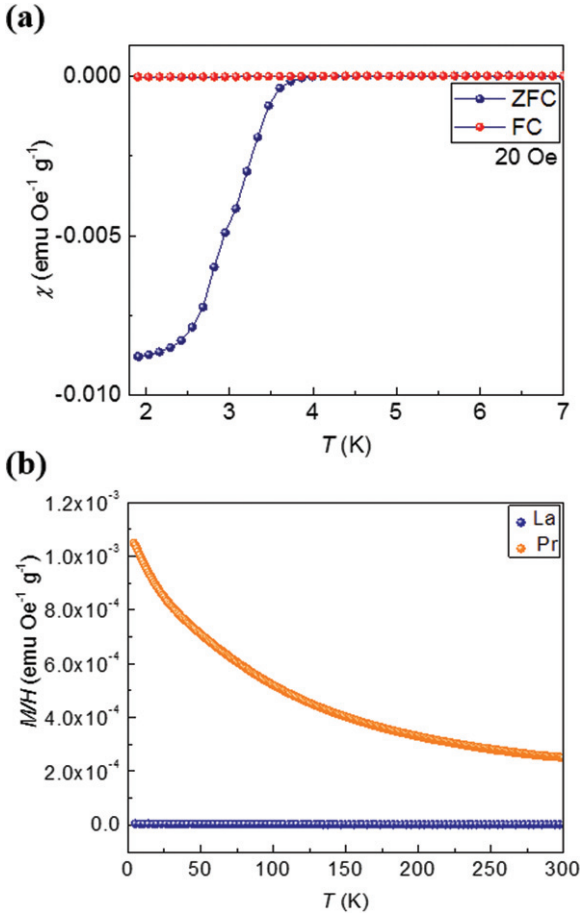

Fig. 4: (a) Temperature dependence of DC magnetic susceptibility for $La_3Cr_{10-x}N_{11}$ with zero field cool (ZFC) and field cool (FC) under a magnetic field of 20 Oe. (b) The normal state susceptibility of $La_3Cr_{10-x}N_{11}$ and $Pr_3Cr_{10-x}N_{11}$.

showing a Curie-Weiss behavior as shown in fig. 4(b). Considering there are no $4f$ electrons occupied by each La^{3+} ion, but two $4f$ electrons occupied by Pr^{3+} ion, we attribute the Curie-Weiss behavior of $\chi(T)$ in $Pr_3Cr_{10-x}N_{11}$ to the magnetic moments of Pr^{3+} $4f$ electrons. Since $La_3Cr_{10-x}N_{11}$ shows superconductivity with no $4f$ electron contributions, we suggest that the superconductivity in both $La_3Cr_{10-x}N_{11}$ and $Pr_3Cr_{10-x}N_{11}$ is due to Cr $3d$ electrons, and the magnetic moments of Cr in those superconductors are close to zero.

Figure 5 shows the specific heat coefficient C/T as a function of T^2 from 2 K to 10 K at zero field. The bulk nature of superconductivity is also confirmed by an obvious specific heat anomaly at $T_c = 4.6$ K, matching well with the resistivity and susceptibility measurements. Because of the exact rigorous synthetic conditions for $La_3Cr_{10-x}N_{11}$, the crystallinity of $La_3Cr_{10-x}N_{11}$ is not better than $Pr_3Cr_{10-x}N_{11}$, and the magnitude of specific heat anomaly at T_c is less than $Pr_3Cr_{10-x}N_{11}$. Since there is Cr_2N impurity phase in the sample, we cannot extract any other useful data such as Sommerfeld constant γ and Debye temperature Θ_D in $La_3Cr_{10-x}N_{11}$. The

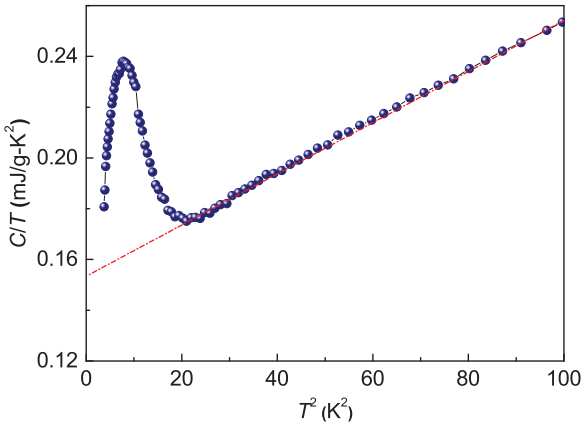

Fig. 5: The low temperature specific heat data in the superconducting regime.

large electronic specific-heat coefficient of 170 mJ/molK^2 in $Pr_3Cr_{10-x}N_{11}$ is about 10 times larger than that estimated by the electronic structure calculation and the main contributions around E_F is from Cr $3d$ electrons in both $Pr_3Cr_{10-x}N_{11}$ and $La_3Cr_{10-x}N_{11}$. So we can deduce that the electronic specific-heat coefficient of $La_3Cr_{10-x}N_{11}$ is the same level around 170 mJ/molK^2. Both of them have strong electron correlations and quantum fluctuations might be involved.

To further investigate the electronic properties, we have carried out first-principles electronic structure calculations on $Ln_3Cr_{10-x}N_{11}$ (Ln = La, Ce, Pr). The primitive cell of $Ln_3Cr_{10-x}N_{11}$ is illustrated in the inset of fig. 6, where two types of nonequivalent Cr atoms are denoted by Cr1 and Cr2, respectively. The local density of states (LDOS) of $Ln_3Cr_{9.5}N_{11}$ is plotted in fig. 6, according to which the contribution from different atomic species can be determined. In $La_3Cr_{9.5}N_{11}$ and $Pr_3Cr_{9.5}N_{11}$ [11], most of contribution around the Fermi level (E_F) comes from the Cr1 and Cr2 atoms, mainly consisting of Cr $3d$ orbitals. In contrast, the states of La/Pr and N atoms contribute much less around E_F. The results do not change very much at a higher density of Cr2 vacancies. According to our calculations, the total DOS of $Ln_3Cr_{9.5}N_{11}$ at the Fermi level N(E_F) is dominated by Cr $3d$ electrons, indicating that the superconductivity originates from the condensation of Cr $3d$ electrons, similar to that of CrAs [30].

Superconductivity in $La_3Cr_{10-x}N_{11}$ shows several distinct characters. Firstly, while a few alloys and intermetallic compounds containing Cr superconductors [31–36] were found where the $4s$ electrons may account for the superconductivity, superconductivity in Cr-based compounds were only reported in arsenide materials. Therefore, $La_3Cr_{10-x}N_{11}$ and $Pr_3Cr_{10-x}N_{11}$ are the only Cr-based superconductors discovered in chromium nitrides. Further theoretical and experimental studies are needed to determine the pairing symmetry and the corresponding mechanism of superconductivity in this material.

Secondly, $La_3Cr_{10-x}N_{11}$ has a relatively large upper critical field $H_{c2}(0) \sim 12.2$ T, exceeding the Pauli limit

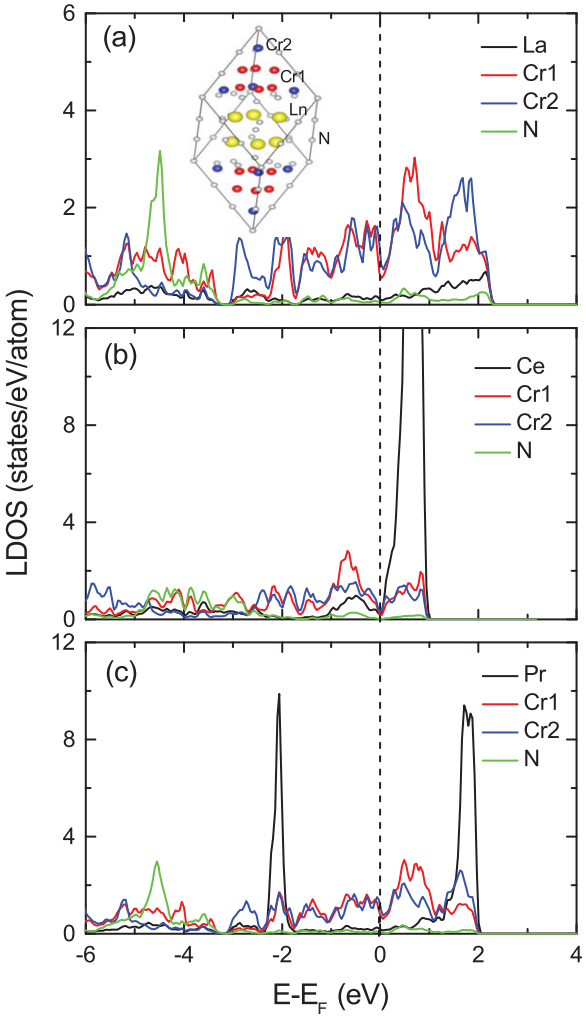

Fig. 6: The local density of states (LDOS) for $Ln_3Cr_{9.5}N_{11}$ (Ln = La, Ce, Pr [11]). The inset shows the primitive cell of $Ln_3Cr_{10-x}N_{11}$ (Ln = La, Ce, Pr).

of paramagnetic pair-breaking field, this is rare in three-dimensional structure superconductors. The remaining puzzle is the high value of $H_{c2}(0)$, which may be accounted for multi-band effect, spin-orbital coupling, or spin-triplet pairing. The H_{c2} of unconventional superconductor $K_2Cr_3As_3$ is three times larger than the Pauli-paramagnetic limit that is regarded as evidence of spin-triplet. It is needed to synthesize higher crystallinity sample or single crystal in the future to explore more details of possibly unconventional superconductivity in $La_3Cr_{10-x}N_{11}$ with Cr 3*d* electrons.

Conclusions. – In conclusion, we report the experimental results for a novel Cr-based superconductor $La_3Cr_{10-x}N_{11}$ with cubic lattice structure. Bulk superconductivity with $T_c \sim 4.6$ K is observed from the resistivity, susceptibility, and specific heat measurements. A large upper critical field is estimated to be about 12.2 T, much larger than the Pauli limit of paramagnetic pair-breaking field. Electronic structure calculations show that most of density of states (DOS) at Fermi energy is contributed by Cr 3d electrons, suggesting the superconductivity is originated from the condensation of Cr 3d electrons. Comparing to $La_3Cr_{10-x}N_{11}$ and $Pr_3Cr_{10-x}N_{11}$, however, $Ce_3Cr_{10-x}N_{11}$ does not show signature of superconductivity above 1.8 K.

* * *

The authors are grateful to Dr. ZhaoYu Liu and Prof. Shi Liang Li (Institute of Physics) for their help in experiments. This work was supported by the National Basic Research Program of China (Grants Nos. 2014CB921500, 2017YFA0302901), the National Science Foundation of China (Grants Nos. 11674375, 11634015, 11774424), the Strategic Priority Research Program and Key Research Program of Frontier Sciences of the Chinese Academy of Sciences (Grant No. XDB07020200), the National Key Research and Development of China (Grants Nos. 2018YFA0305702, 2016YFA0300303).

REFERENCES

[1] Wu W., Cheng J. G., Matsubayashi K., Kong P. P., Lin F. K., Jin C. Q., Wang N. L., Uwatoko Y. and Luo J. L., *Nat. Commun.*, **5** (2014) 5508.
[2] Kotegawa H., Nakahara S., Tou H. and Sugawara H., *J. Phys. Soc. Jpn.*, **83** (2014) 093702.
[3] Cheng J. G. and Luo J. L., *J. Phys.: Condens. Matter*, **29** (2017) 383003.
[4] Bao J. K., Liu J. Y., Ma C. W., Meng Z. H., Tang Z. T., Sun Y. L., Zhai H. F., Jiang H., Bai H., Feng C. M., Xu Z. A. and Cao G. H., *Phys. Rev. X*, **5** (2015) 011013.
[5] Tang Z. T., Bao J. K., Liu Y., Sun Y. L., Ablimit A., Zhai H. F., Jiang H., Feng C. M., Xu Z. A. and Cao G. H., *Phys. Rev. B*, **91** (2015) 020506.
[6] Tang Z. T., Bao J. K., Wang Z., Bai H., Jiang H., Liu Y., Zhai H. F., Feng C. M., Xu Z. A. and Cao G. H., *Sci. China Mater.*, **58** (2015) 16.
[7] Mu Q. G., Ruan B. B., Pan B. J., Liu T., Yu J., Zhao K., Chen G. F. and Ren Z. A., *Phys. Rev. B*, **96** (2017) 140504.
[8] Liu T., Mu Q. G., Pan B. J., Yu J., Ruan B. B., Zhao K., Chen G. F. and Ren Z. A., *EPL*, **120** (2017) 27006.
[9] Mu Q. G., Ruan B. B., Pan B. J., Liu T., Yu J., Zhao K., Chen G. F. and Ren Z. A., *Phys. Rev. Mater.*, **2** (2018) 034803.
[10] Shao Y. T., Wu X. X., Wang L., Shi Y. G., Hu J. P. and Luo J. L., *EPL*, **123** (2018) 57001.
[11] Wu W., Liu K., Li Y. J., Yu Z.-H., Wu D. S., Shao Y. T., Na S. H., Li G., Huang R. Z., Xiang T. and Luo J. L., to be published in *Natl. Sci. Rev.* (2019) DOI:10.1093/nsr/nwz129.
[12] Broll S. and Jeitschko W., *Z. Naturforsch. B*, **50** (1995) 905.
[13] Goodenough J. B., Longo J. M. and Kafalas J. A., *Mater. Res. Bull.*, **3** (1968) 471.
[14] Toby B. H., *J. Appl. Cryst.*, **34** (2001) 210.
[15] Blochl P. E., *Phys. Rev. B*, **50** (1994) 17953.

[16] Kresse G. and Joubert D., *Phys. Rev. B*, **59** (1999) 1758.
[17] Kresse G. and Hafner J., *Phys. Rev. B*, **47** (1993) 558.
[18] Kresse G. and Furthmuller J., *Comput. Mater. Sci.*, **6** (1996) 15.
[19] Kresse G. and Furthmuller J., *Phys. Rev. B*, **54** (1996) 11169.
[20] Perdew J. P., Burke K. and Ernzerhof M., *Phys. Rev. Lett.*, **77** (1996) 3865.
[21] Dudarev S. L., Botton G. A., Savrasov S. Y., Humphreys C. J. and Sutton A. P., *Phys. Rev. B*, **57** (1998) 1505.
[22] Werthamer N. R., Helfand E. and Honenberg P. C., *Phys. Rev.*, **147** (1966) 295.
[23] Clogston A. M., *Phys. Rev. Lett.*, **9** (1962) 266.
[24] Chandrasekhar B. S., *Appl. Phys. Lett.*, **1** (1962) 7.
[25] Gurevich A., *Phys. Rev. B*, **67** (2003) 184515.
[26] Carbotte J. P., *Rev. Mod. Phys.*, **62** (1990) 1027.
[27] Lee I. J., Chaikin P. M. and Naughton M. J., *Phys. Rev. B*, **62** (2000) 14669.
[28] Liu Y., Wang Z. Q., Zhang X. F., Liu C. F., Liu Y. J., Zhou Z. M., Wang J. F., Wang Q. Y., Liu Y.Z., Xi C. Y., Tian M. L., Liu H. W., Feng J., Xie X. C. and Wang J., *Phys. Rev. X*, **8** (2018) 021002.
[29] Tinkham M., *Introduction to Superconductivity*, 2nd edition (Krieger Pub. Co., New York) 1996.
[30] Autieri C. and Noce C., *Philos. Mag.*, **97** (2017) 3276.
[31] Matthias B. T., Compton V. B., Suhl H. and Corenzwit E., *Phys. Rev.*, **115** (1959) 1597.
[32] Matthias B. T., Geballe T. H., Compton V. B., Corenzwit E. and Hull G. W., *Phys. Rev.*, **128** (1962) 588.
[33] Bucher E., Muheim J., Heiniger F. and Muller J., *Rev. Mod. Phys.*, **36** (1964) 146.
[34] Andres K., Bucher E., Maita J. P. and Sherwood R. C., *Phys. Rev.*, **178** (1969) 702.
[35] Smith T. F., *J. Low Temp. Phys.*, **6** (1972) 171.
[36] Niimura H., Kawashima K., Inoue K., Yoshikawa M. and Akimitsu J., *J. Phys. Soc. Jpn.*, **83** (2014) 044702.